Study of the vortex dynamics in a mechanical model of the vocal folds using Particle-Image Velocimetry

Christoph Bruecker[1], Michael Triep[1], Malte Kob[2]

[1]Aerodynamisches Institut, RWTH Aachen, Germany
[2]Universitätsklinikum Aachen, Klinik für Phoniatrie, RWTH Aachen, Germany
bruecker@aia.rwth-aachen.de

Abstract

The intention of the present study is the detailed analysis of the unsteady vortex dynamics downstream the human glottis during phonation at typical fundamental frequencies. A hydraulic respiratory mock circuit has been built-up including a three-times up-scaled realistic dynamic model of the vocal folds. The function of the human glottis is reproduced by two counter-rotating cams each of which is covered with a stretched silicone membrane. The 3-D geometry of the cams is designed such that the rotation leads to a realistic time-varying motion and profile of the glottis and waveform of the glottal cycle. The unsteady velocity and vorticity dynamics is measured using High-Speed PIV. The results help to understand the vortex-induced noise generated in human voice. In addition, changing the 3-D contours of the cams in different specific ways enables to investigate basic pathological differences of the glottis function and the resulting alterations of the velocity and vorticity field in the vocal tract.

1. Introduction

The voice generation in the larynx (see Fig. 2) is mainly due to the pulsating flow through the glottis generated by the passive vocal fold vibration. The interaction between the elastic and muscular tension contained in the stretched vocal folds and the aerodynamic forces define the crucial voice parameters, e.g. the fundamental frequency, the intensity level and the voice quality.

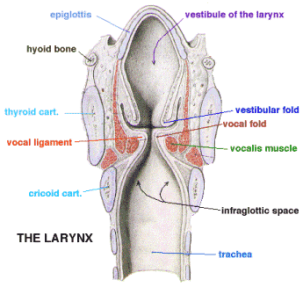

Fig. 1: *Anatomy of the larynx (webpage of the Center For Laryngeal and Voice Disorders, The Johns Hopkins University School of Medicine),*

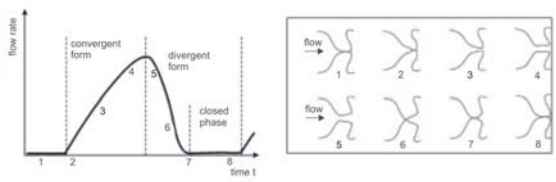

Fig.2: *Typical waveform of glottal volume flow for a full phonation cycle and the characteristic variation of cross-sectional glottal profile (right) (Hirano et al., 1987)*

At the beginning of a phonation cycle the glottis is closed and the vocal folds are stretched. Air pressure builds up in the trachea against the folds until these no longer can withstand the force and allow air to pass between (see Fig. 2). The consequential decrease of sub- and transglottal pressure as well as the elastic restoring force of the vocal folds cause the anew closure of the glottis. The pressure is built-up in the trachea once more and the phonation cycle is repeated, so that on the whole the vocal folds carry out a self-sustained periodic oscillation. In Fig. 2 (right) it is indicated that the glottis converts from a fully convergent duct in the opening phase (2-3) over a brief parallel phase (4) into a divergent duct in the closing phase (5-6). As a consequence the separation point of the emerging free jet is in constant move. Furthermore within the divergent phases of the glottis the free jet is prone to reattach at one of the duct walls (Coanda effect, see Pelorson et al. 1994 and Hirschberg et al. 1996), which may lead to an asymmetric inflow into the vocal tract. The effects of the free jet are mainly responsible for noise generation which will be superposed to the fundamental frequency and the high-frequency components. This additional noise source is one of the reasons that the human voice differs from that of a synthetic voice.

Up to now there is still a lack of detailed knowledge of the transient flow downstream of the glottis. Hot-wire anemometry and pressure measurements were carried out by Barney (1995) in a dynamical model of the vocal folds, which was composed of two externally driven shutters that oscillated in a simple duct. Vilain (2001) has modeled the vocal folds by two water-filled latex tubes that could be adjusted through pressure for asymmetric cases. His set-up reproduced self-sustained oscillations very similar to speech in normal and pathological phonation. He focused mainly on pressure measurements. First simplified numerical simulations of glottal flow were reported by Liljencrants (1991). Frankel et al. were the first to present results of CFD simulation of the 2-D unsteady flow in the glottis with a dynamically changing gap width. All published experimental work however does not take into account the change of the glottis profile which is modeled herein. In addition, only spatial and temporal resolving measurements methods as time-resolved PIV are able to investigate the complex vortex dynamics related with the free jet to understand the noise generation.

2 Experimental model and set-up

2.1 The mechanical model

A new model approach was designed to reproduce the physiological time-varying motion and profile of the glottis. Two cams are pivoted with two respective wedges that reproduce the inlet angles of 45° and the exit angles of 10° from the glottal duct. The vocal folds are mimicked by silicone membranes that are deformed by these symmetrically arranged cams. Each of the wedges pivoting one of the cams is covered with such a stretched silicone membrane (see Fig.3 left). The main function of these membranes is to adapt themselves continuously to the shape of the cams and the inlet and outlet geometry. One second convenience of the membranes is that they seal the channel inside to the outside world without leakage.

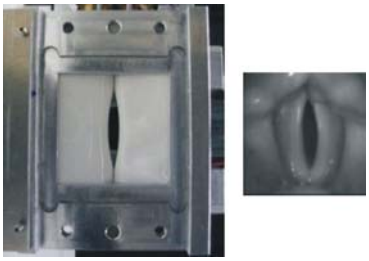

Fig. 3: *Photographic view of the glottal model developed for this study (left) vs. laryngoscopic view of the human vocal folds at maximum opening (right, taken from http://www.phoniatrie.uni-erlangen.de)*

As the cams are brought near together and move in counter-rotation, the cross-section in the gap between both silicone membranes is varying according the specific 3-D profile contours of the cams. In order to achieve a similar characteristic time-varying motion and profile of the glottis as observed in the human folds the cams have a 3-D profile contour with an near-elliptic cross-section in the middle and a circular cross-section at both ends, generated by CAD and manufactured on a 5-axis milling machine. A comparison of the mechanical glottis and a human glottis in fully open position is shown in Fig. 3. Using different cams with different profile contours or different rotation speeds one can simulate also the principle typical pathological dysfunction of the human vocal folds. Therefore we are able to mimic the complex movement of the vocal folds by a simple rotational movement.

The model is three-times enlarged in comparison to the human vocal folds and is used in a water channel to take advantage of the strongly reduced characteristic frequencies and velocities. With the Reynolds- and the Strouhal number constant for the original and the mechanical model, the frequency is reduced by a factor of 135 and the typical flow velocities are of order of 1 m/s. This allows detailed flow studies using optical whole-field measurements techniques like Particle Image Velocimetry (PIV).

2.2 The flow channel

The experimental set-up consists of an hydraulic set-up including the vocal folds unit, a drive-train unit, an optical set-up and the high-speed imaging and processing system. The following table gives an overview of the typical geometric and fluid-dynamical data for the vocal folds of healthy test persons:

height of the trachea H	18 – 22 mm
length of the vocal folds l_G	14 – 22 mm
thickness of the vocal folds b	3 – 6 mm
maximal glottal width w_{max}	1 – 3 mm
pressure difference across the glottis Δp_G	500 – 2000 Pa
mean velocity through the glottis u_{mean}	20 – 40 m/s
Fundamental frequency of the oscillation f	100 – 200 Hz

Table 1: *Characteristic numbers of the relevant physiological parameters (Pelorson et al. 1994)*

During phonation the vocal folds form a gap (glottis) about 2 mm wide which is about 10% of the vocal folds length. This fact allows us to investigate the glottal flow in a channel with a square cross section. The characteristic dimensionless numbers of the present problem built with average values from Table 1 and yield Ma = $O(10^{-1})$, Sr = $O(10^{-2})$, Re = $O(10^{3})$. The flow may therefore be regarded as incompressible (compact sound sources). Down to the glottis we are dealing with a laminar character of the flow. Further downstream the flow detaches from the vocal folds giving rise to a turbulent free jet through the consecutive false vocal folds into the vocal tract. Even if the Strouhal number presumes a quasi-steady flow, the unsteady effects due to the opening and closing of the glottis are of relevance to the formation of the vortex structures and may not be neglected in the present problem. In fact, the detaching vortex structures and their characteristic frequencies are the more physical relevant time-scales compared to the fundamental oscillation frequency .

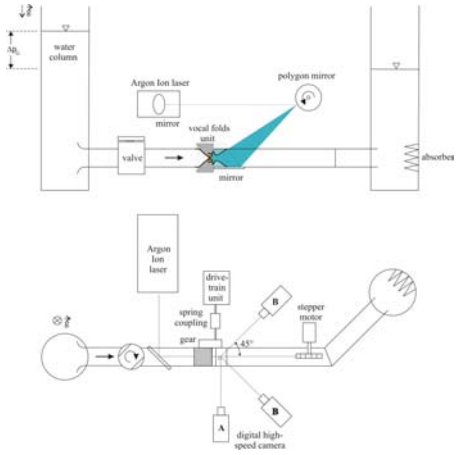

Fig. 1: Front- and top view of the experimental set-up

The three-times up-scaled model of the glottis is 60 mm high and has a maximal gap width of 8 mm. It is located at the downstream end of the inlet channel which has a square cross section of 60 mm x 60 mm representing the model trachea. The upstream side of the model trachea is connected to a reservoir which provides a constant subglottal pressure, that is the expiratory pressure of the lung. For the cycle-resolved measurements the pressure difference of □pG = 6 cm WS across the glottis is kept constant by continuously refilling the upstream column so that equal conditions are provided for each consecutive glottal cycle.

Immediately downstream of the human vocal folds there is a second constriction, the so-called false vocal folds which presumably play an additional important role in the fluid dynamics of the glottal flow and should therefore also be included in any model geometry of the vocal tract. For our studies, the false vocal folds were created from perspex according to the statistical data published by Agarwal et al. (2003) and were fixed inside the channel walls as a second constriction, see Fig. 5. It shows a close-up view and the relative scales to the true vocal folds.

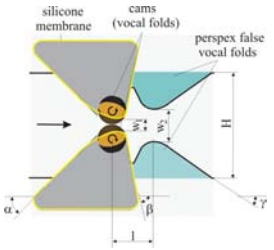

α	45°
β	80°
γ	35°
$(w_1)_{max}$	8 mm
$w_2/(w_1)_{max}$	2.25
H	60 mm
l/H	0.40
l_G	48 mm

Fig. 5: *Close-up view of a cut through the vocal folds unit and model dimensions*

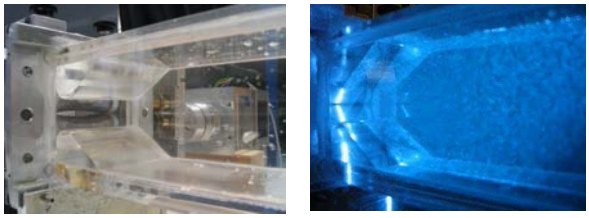

Fig. 6: *Oblique photographic view upon the vocal folds unit through the unfilled channel (left) and under experimental conditions*

The straight transparent channel downstream of the glottis represents the vocal tract which ends into a second column forming altogether a U-shaped system of two communicating columns. At half way of the vocal tract, the channel is redirected about an angle of 45° which was considered for two reasons: the avoidance of pressure wave reflections which will be finally absorbed at the end, and the additional optical access for frontal viewing into the glottis. Finally, Fig.6 gives an impression of the centre-piece of the flow channel, the vocal folds including the false vocal folds, photographed with an empty and a water-filled vocal tract.

Both cams are driven by one single gear which itself is connected by an interposed spring coupling to an indexing cam gear which reproduces the open and closed phases encountered in the physiological waveform of the glottal cycle (see Fig. 2 right). Fig. 7 demonstrates the physical variation of the channel geometry from a convergent profile to a divergent profile including an up- and downstream displacement of the smallest cross-section when having an elliptical cross-section of the cams. The open quotient for a vocal cycle in this study is exactly 50%.

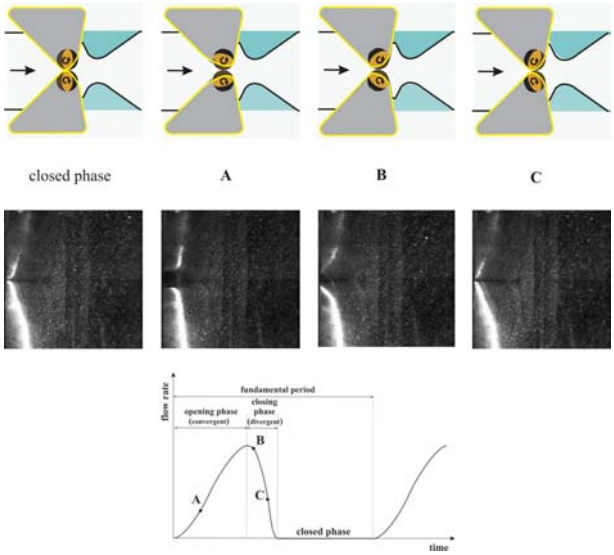

Fig. 7: *Time dependence of the flow rate for one glottal cycle (bottom) and three selected characteristic phase points with respective cams angular position highlighted (middle and top).*

2.3 Optical arrangement

The technique of time-resolving high-speed PIV is used to measure the spatial and temporal evolution of the flow field. Therefore, a digital high-speed camera (Weinberger, Speedcam 512) is used which runs with 1024 fps at a resolution of 512 x 512 and records the flow in the light-sheet plane. The beam of a 8 Watt continuous Argon-Ion laser (COHERENT Innova 90) is expanded to a virtual light-sheet using a polygon mirror, which redirects the laser beam during rotation in flow direction and illuminates the flow with each passing facet. The scanning frequency is adapted to the highest expected flow velocities so that acceptable spatial resolutions are still possible for the correlation. A main feature of the recording camera is that it permits to exactly record a certain frame sequence starting at any desired phase point for several consecutive glottal cycles what is necessary for phase-averaged measurements. The trigger signal for the camera is provided by a National Instruments Counter Card that is itself fed with two different optical barrier signals, one from the polygon mirror and the other from the cam-driving gear .

3. Results

The first experiments were carried out with a single high-speed camera, see position A in Fig. 4. The camera is oriented normal to the light sheet plane which illuminates the flow in the centre plane. The recording is synchronized with the polygonal mirror and triggered with an optical barrier at the cam gear. A specialized electronics allows the gating of the

high-speed camera such that sequences of frames can be recorded at any desired phase position in the vocal cycle for a large number of successive cycles.

We focus here on 3 characteristic phase positions as depicted in Fig. 7. Phase A is the opening of the glottis when the glottis profile resembles a smooth convergent constriction. At phase B the glottis is already in the closing phase with a divergent form. In between these phase positions, the glottis has parallel walls for a short moment. Finally, phase C corresponds to the moment short before complete closure of the glottis. For all 3 phases we recorded over 100 successive cycles to analyze the phase-averaged flow fields and the cycle-to-cycle variations. The results (Fig. 8) are presented in the following form: the left column represents phase-averaged results and starts at the top with the profile of the axial velocity component and the phase-averaged velocity field in the centre plane. Below these, the fluctuating intensities and structure is given by contour lines of the rms values of the velocity relative to the mean axial velocity. At the bottom one can see the distribution of the vorticity component normal to the light-sheet plane; the right column displays several selected instantaneous flow pictures to demonstrate the cycle-to-cycle variations of the flow pattern.

Phase A: The phase-averaged flow field shows the formation of a jet-like flow which is entering the vocal tract. The phase-averaged flow field is approximately symmetric to the centreline while the instantaneous pictures display a strong cyclic variation which is explained by the Coanda effect. The jet is partly attached to the upper wall of the upper false vocal fold and vice versa. The maximum axial velocities reach values of about 0.5 of umean in the smallest gap between the false vocal folds at x/H 0.4. This is also the area of highest fluctuations at the centre of the jet.

Phase B: This phase is characterized by a strong second jet which is overtaking the first jet. This jet has a cone-like shape at its front as well seen in the velocity vector field. The maximum velocities are about a factor of 3 higher than in phase A reaching values of 1.5 umean. Surprisingly this second strong jet is formed in the phase when the gap width is already decreasing and the channel profile becomes divergent. The above described feature is characteristic for the given temporal evolution of the glottis profile. The areas with the highest fluctuations are found on the lateral sides of the cone-like front of the jet at x/H 0.6 and y/H ±0.15 as seen by the local maxima in the contour plot. From the velocity profile along the centreline we estimate the front propagation speed of the jet to a value of 0.21m/s. Calculated back to the original values in the larynx one obtains front propagation speeds of about 9.5 m/s.

Phase C: The flow in phase C is the moment before the glottis is closed. The strong jet has diminished and broadened in size. Large recirculation zones can be seen at the outlet wall regions in the vocal tract. The maximum velocities are again decreased to values of about 0.5 umean and the forward flow is limited to the centre region within a width of y/H ±0.25. This boundary region of the jet is also the source for high intensity fluctuations and high vorticity as typical for the shear layer of a jet. The instantaneous pictures let recognize the roll-up of vortices in the shear layer and the formation of larger coherent vortex structures. However, the coherence is disturbed because of the remaining flow disturbances after glottis closure which is the initial downstream condition for the next cycle.

4. Summary and Outlook

The aim of this study was a first look at the time-dependant flow patterns occurring in the vocal tract, especially the built-up and decay of the free jet downstream of the oscillating vocal folds during several consecutive glottal cycles. For this purpose a larynx model, including true and false vocal folds, was built-up. The main characteristics of the model were the realistic reproduction of time-varying motion and profile of the glottis and waveform of the glottal cycle. Future work on the flow channel includes the measurements of the pressure distribution on the walls of the vocal tract and the correlation of the pressure signals with the vortex dynamics. In addition, the measurement of the time-resolved velocity distribution allows to calculate the internal pressure field from the Poisson equation for the pressure, deduced in a first approximation from the Navier-Stokes equations for a 2-D unsteady viscous flow. This will give more information on the sources of any additional noise in human speech.

Acknowledgement

The first author gratefully acknowledge the support of this project by the Deutsche Forschungsgemeinschaft grant no. BR 1494/4-1.

5. References

Agarval M, Scherer R, Hollien H: The false vocal folds: shape and size in frontal view during phonation. *Journal of Voice* 17, no. 2, 2003.

Barney A: luid flow in a dynamic mechanical model of the larynx. PhD thesis University of Southampton, 1995.

Frankel S et al.: webpage at http://ristretto.ecn.purdue.edu/research/biological_flows.htm

Hirano M, Yoshida T, Kurita S: Anatomy and behavior of the vocal process. In: *Laryngeal function in phonation and respiration*. Baer T., Sasaki C., Harris K. Ed. 1-13. College Hill Press, Boston, 1987.

Hirschberg A, Pelorson X, Hofmans G, Hassel R, Wijnands, P: Starting transient of the flow through an in-vitro model of the vocal folds. In: *Vocal fold physiology*: *Controlling complexity and chaos*. Davis, P.J.; Fletcher, N.H. (editor), Singular Pub. Group, San Diego, 31-46, 1996.

Liljencrants J: Numerical simulations of glottal flow. Proc. Eurospeech 91, Vol. 1, 255-258, Genova 1991.

Pelorson X, Hirschberg A, van Hassel RR, Wijnands APJ: Theoretical and experimental study of quasisteady-flow separation within the glottis during phonation. Application to a modified two-mass model. *J. Acoust. Soc. Am.* 96 (6), 3416-3431, 1994.

Vilain C, Pelorson X, Hirschberg A, Willems JFH, Le Marrec, L: Study of the airflow through in-vitro oscillating pathological vocal folds. Proc. 2nd Int. Workshop on Models and Analysis of Vocal Emissions for Biomedical Applications (MAVEBA), A. Manfredi (editor), University Florence, Italy, 2001.

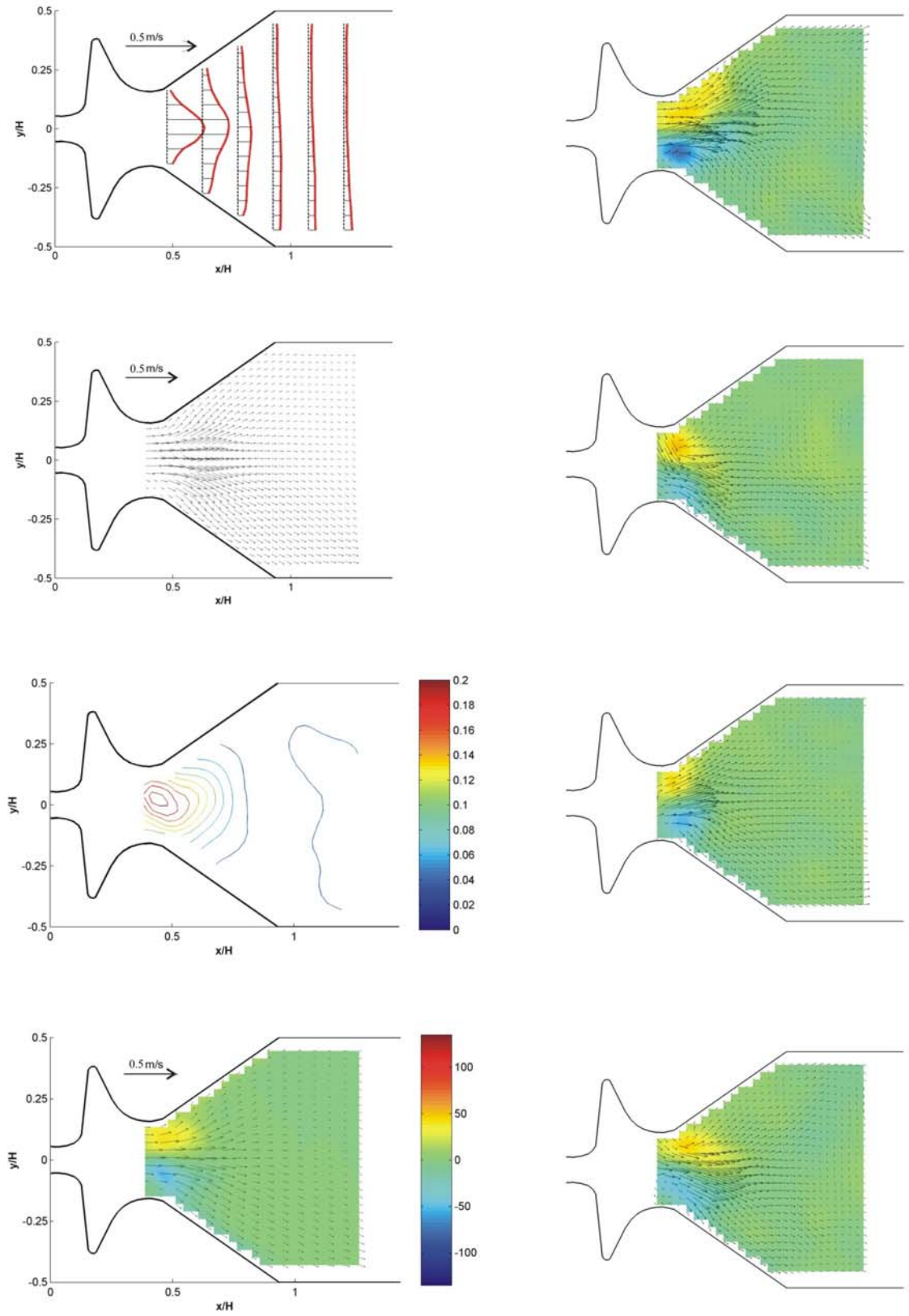

Fig. 8: *Phase-averaged flow field (left column) and exemplars instantaneous pictures (right column) downstream of the glottis in the midplane at a given phase position in the vocal cycle: phase A.*

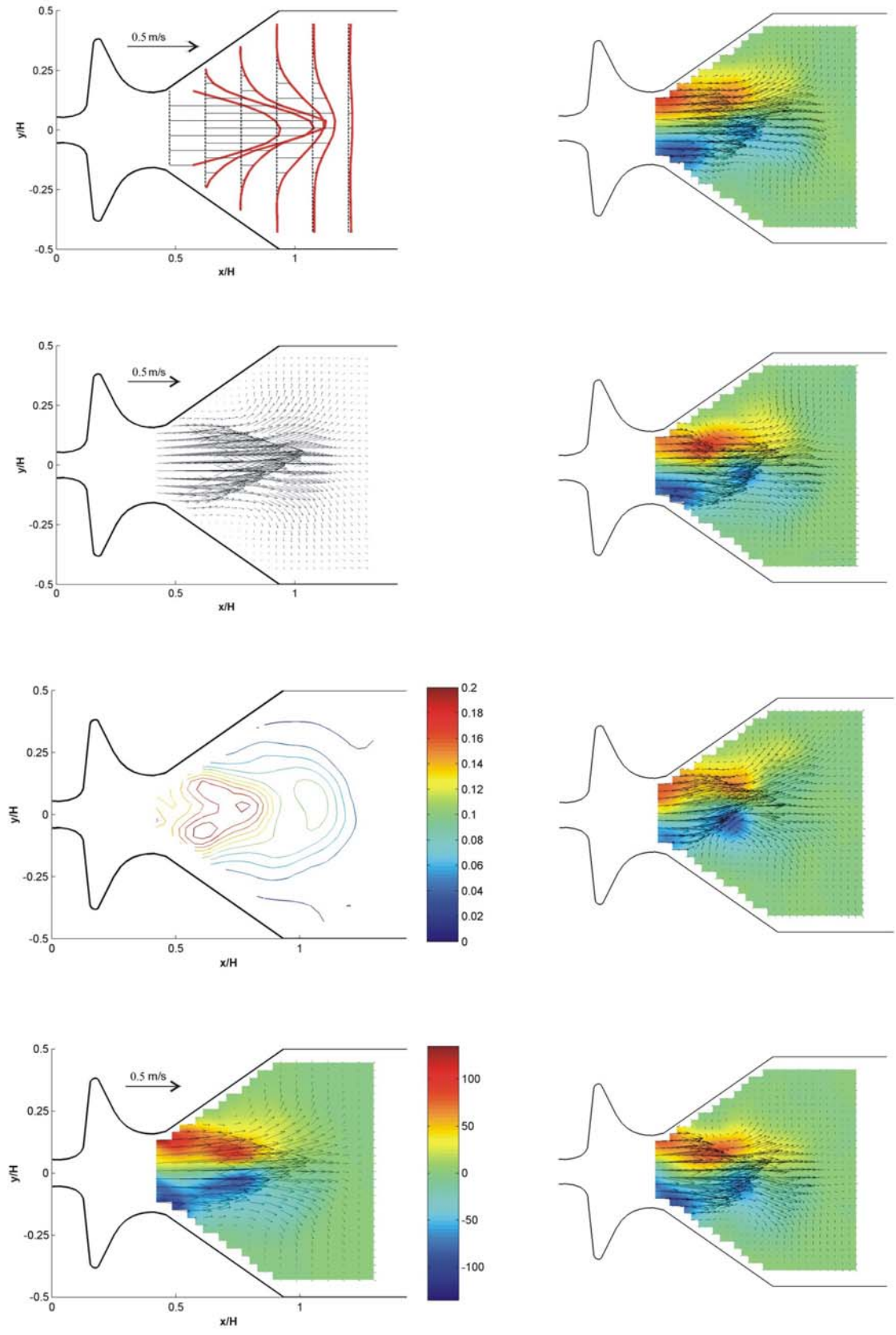

Fig. 8: *Cont'd: phase B.*

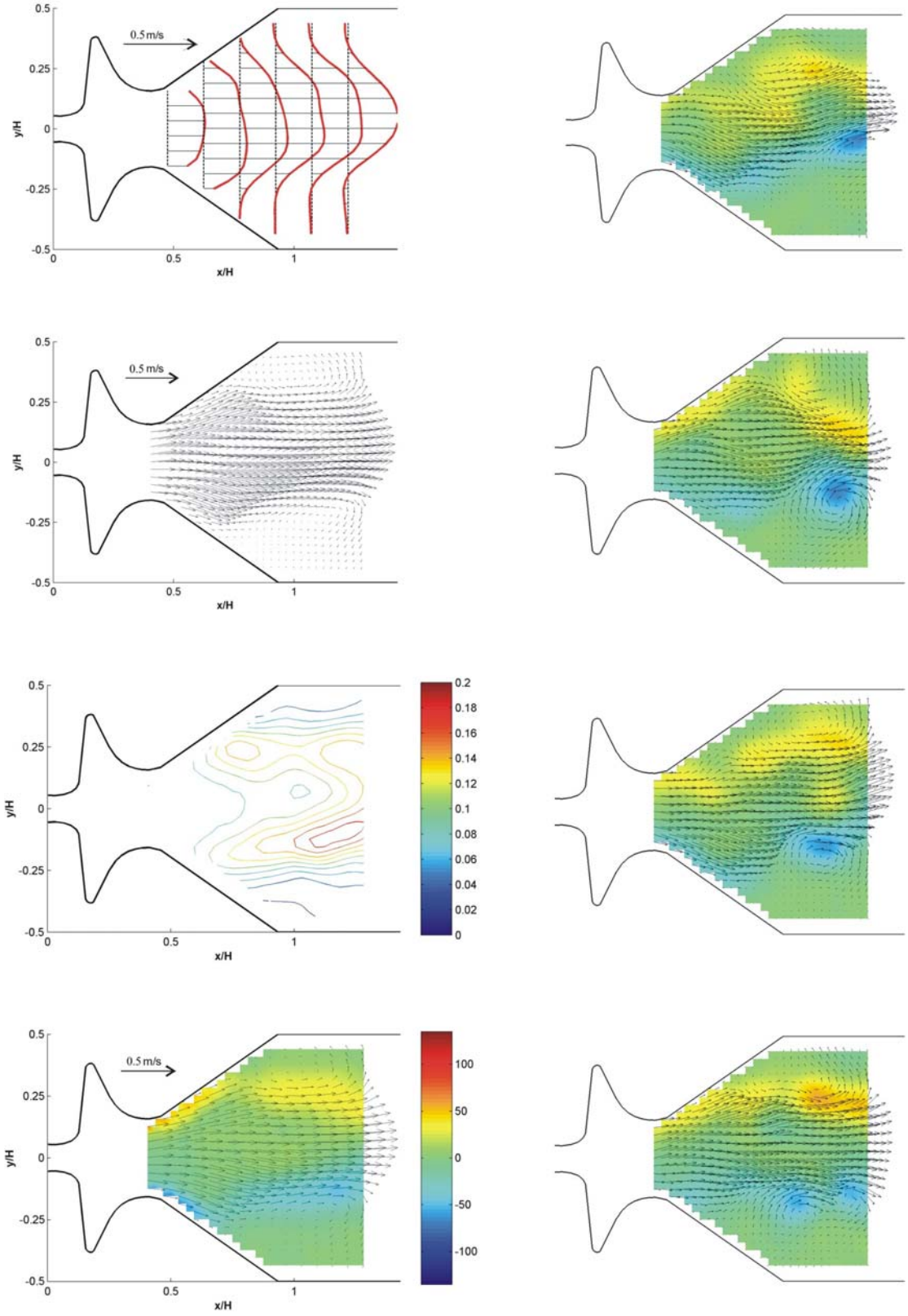

Fig. 8: *Cont'd: phase C.*